AUTOMATED DATA COLLECTION IN FRAGMENTATION WARHEAD TESTS

M.F. Maritz[1], C.J. Terblanche[2] and G.J.F. Smit[1]

[1]Department of Mathematical Sciences, Division Applied Mathematics, University of Stellenbosch, Private Bag X1, Matieland, South Africa, ZA 7602.
[2]DENEL Land Systems, Western Cape, PO Box 187, Somerset West, South Africa, ZA 7129.

The semi-automation of acquiring position coordinates and other relevant data of holes in witness plates using image processing techniques as well as Fourier shape description techniques is presented. In particular Fourier shape description is used to automatically classify holes as regular (resulting from a simple perforation) or irregular (resulting from multiple perforations) in order that the irregular holes can be manually cut into supposed single perforations by the user.

INTRODUCTION

The availability of suitable digital image acquisition equipment opens new possibilities for diagnostic analysis in ballistics research (see e.g. [1], [2], [3]). With this comes the need for image processing techniques in order to extract the required data from digital images and ballistic researchers will undoubtedly apply and tailor some of the existing processing techniques for their own applications (e.g. [4]).

Two main sources of images in ballistic research are visible light images and flash radiographs. The former can be obtained by a digital camera and applications may include the analysis of holes in billets from impact tests, and holes in witness plates used in fragmentation warhead tests. The latter may be obtained by newly available X-ray scanners (see e.g. [1], [5]) and applications may include analysis of particles in flash radiographs of particulated shaped charge jets, or the fragments in radiographs of fragmentation warhead tests.

Shape analysis of 2D shapes in an image as a post processing phase after distortion removal, equalization, segmentation and boundary extraction, [6], [7], [8], can invariably add value to the data extraction process. The most basic measurement required is the position coordinates of the centroid of each shape. However, more

1243

detailed shape analysis often can supply more information, such as the mean length, mean width and orientation of elongated shapes. There is often also the requirement to classify and count various shape types, and for large numbers of shapes per image the need for automation is more importunate.

Fourier shape description offers an easy and robust method for performing this task. It has been used mainly in the literature on biological research for shape comparison and classification ([9] is a typical example). However, it does not appear to have been used frequently in the ballistics research, and it is the aim of this paper to illustrate the use of Fourier shape description in an application of semi-automated witness plate analysis. We shall, however, discuss shape analysis in a more general way.

For shape analysis the relevant shapes first need to be segmented out, i.e. a binary image must be obtained that contains the shapes as individual patches [6, Chapter 10]. Then a suitable boundary parameterization method must be applied to obtain the boundaries. Alternatively these two processes may be combined in the form of active contour parameterisation, such as 'snakes' [10] or geodesic active contours [4]. This paper assumes that suitable segmentation and boundary parameterisation have been done, and that each shape is available as an ordered set of points on a closed curve in the observation plane.

Figure 1 shows a monochrome digital image of a section of a typical witness plate used in fragmentation warhead tests. In order to assess the performance of the warhead, the following data is required for each simple hole: position coordinates of the centroid, area, length, width, and orientation angle with respect to the horizontal. In order to collect the required data, the image is segmented using a standard segmentation method. The area of each segmented hole in square pixels as well as the boundary of the hole is obtained by boundary tracing.

The required parameters for simple holes are obtained from the parameterized boundary. Fourier shape description is used here to obtain the orientation angle. This will be described in the next section.

However, compound holes resulting from overlapping multiple perforations provide a problem. These compound holes must first be hand separated into their supposed simple perforations, and thereafter each simple perforation is analysed in the normal way. Fourier shape description is used here to classify holes automatically into regular and irregular holes. A small software application was developed that finds the irregular holes automatically and then prompts the user to hand separate only the irregular holes. The data for regular holes are automatically calculated and stored. This process amounts to substantial savings in human operator time since the operator does not need to visually scan the image for possible compound holes.
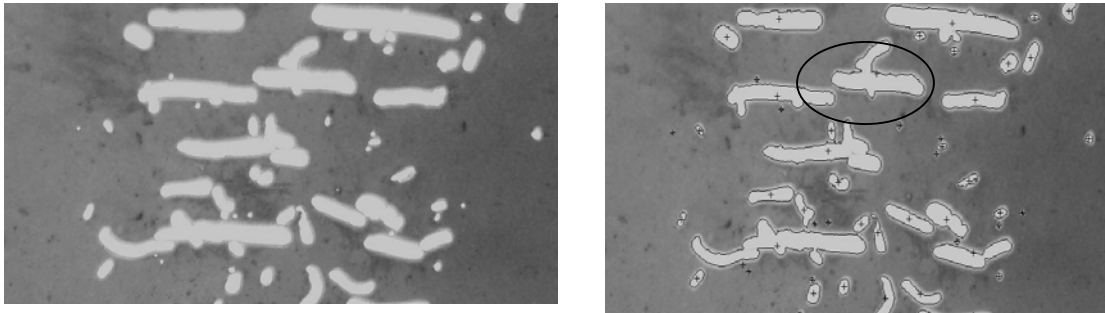
Figure 1. Left: An image of a section of a perforated witness plate. Right: After segmentation and boundary tracing, also showing the edge centroids denoted by +. The encircled hole is used further on for illustration purposes.

FOURIER SHAPE DESCRIPTION

Consider a general closed curve obtained from boundary tracing of a patch in a binary image. Let the coordinates of the boundary be given by (x_j, y_j), $j=1,...,N$. Note that for boundaries obtained from images, the basic length unit is one pixel width, and these coordinates are then supplied as integers.

Although Fourier transformation can be applied to the x and y coordinates separately, it is convenient to do the transformation simultaneously as a single complex variable. We therefore consider the closed curve to lie in the complex plane and be given by

$$z_j = x_j + i\, y_j, \qquad\qquad j = 0,1,...,N-1, \qquad\qquad (1)$$

where $i = \sqrt{-1}$.

The Discrete Fourier Transform (DFT) of z_j is given by

$$\hat{z}_m = \sum_{j=0}^{N-1} z_j \exp(-2\pi\, ijm/N), \qquad m = 0,1,...,N-1. \qquad (2)$$

The values $\hat{z}_m$ will be referred to here as the *Fourier coefficients* in the expansion. The closed curve z_j may be recovered from $\hat{z}_m$ by applying the Discrete Inverse Fourier Transform (DIFT),

$$z_j = \frac{1}{N} \sum_{j=0}^{N-1} \hat{z}_m \exp(2\pi\, ijm/N), \qquad j = 0,1,...,N-1. \qquad (3)$$

Both transforms may be computed efficiently by using the Fast Fourier Transform (FFT) algorithm [11].

Note that in this formulation the high frequencies are represented by coefficients in the middle of the range and low frequencies come from coefficients at the ends of the range. For example the first mode is represented by coefficients $\hat{z}_1$ and $\hat{z}_{N-1}$, the second mode is represented by coefficients $\hat{z}_2$ and $\hat{z}_{N-2}$. Most computer software packages return the DFT (or FFT) in this form.

Because of the periodicity in the coefficients, negative indices also make sense, for example by setting $m = -1$ in (2), the coefficient $\hat{z}_{-1}$ is obtained, but this is equal to $\hat{z}_{N-1}$. In general $\hat{z}_p = \hat{z}_{p+kN}$ for $p, k \in Z$, and we shall henceforth use this more symmetric formulation and, for example, refer to the coefficients of the k-th mode as $\hat{z}_k$ and $\hat{z}_{-k}$.

Approximations of the closed curve are obtained when the higher frequencies are omitted in the DIFT, and only frequencies up to mode M are retained, i.e.

$$\widetilde{z}_j = \frac{1}{N} \sum_{j=-M}^{M} \hat{z}_m \exp(2\pi\, ijm/N), \qquad j = 0,1,...,N-1. \tag{4}$$

Figure 2 shows some approximations of the encircled hole in Figure 1 for various values of M. The case $M = 0$ represents a point at coordinates (X, Y) where X and Y are the means of the respective coordinates. It denotes the *edge centroid*, and may be used as an estimate of the *area centroid* of the shape. Note that for fragment shadows obtained from radiographs, the shape is a projection of a 3D fragment and the researcher actually needs the coordinates of the *volume centroid* (i.e. the barycentre) of the 3D fragment. However, relative to the general scale of the domain in which fragments fly, fragments are small and other errors dominate the measurement process, so that for practical purposes the three different centroids are close enough so that any one may be used as an estimate of the other.
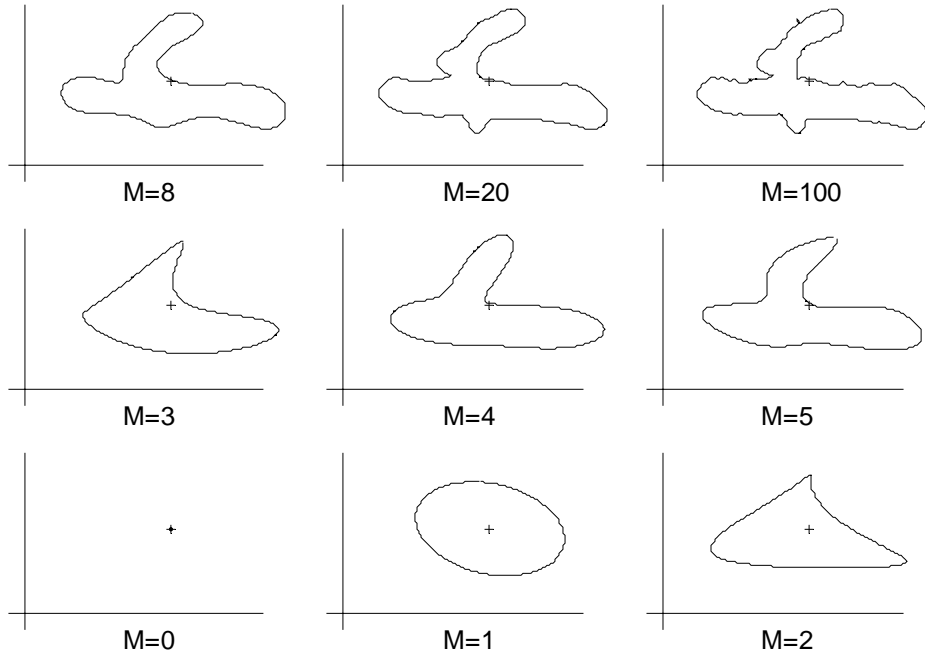
Figure 2. Shape approximations of the encircled shape in Figure 1 for various values of *M*.

Of particular importance is the *approximation ellipse*, given by (4) with $M = 1$. This curve is a rotated ellipse centred at the (X, Y) where

$$\hat{z}_0 = X + iY . \tag{5}$$

The ellipse has semi-axes given by

$$a = \frac{|\hat{z}_1| + |\hat{z}_{-1}|}{N}, \qquad \text{and} \qquad b = \left| \frac{|\hat{z}_1| - |\hat{z}_{-1}|}{N} \right|, \tag{6}$$

where the vertical bars denote the modulus: $|z| = \sqrt{x^2 + y^2}$. The major axis of the ellipse makes an angle θ with respect to the horizontal, where

$$\tan(2\theta) = \frac{\mathrm{Im}(\hat{z}_{-1}\bar{\hat{z}}_1)}{\mathrm{Re}(\hat{z}_{-1}\bar{\hat{z}}_1)} . \tag{7}$$

The overbar denotes the complex conjugate: $\bar{z} = x - i\,y$. The area of the approximation ellipse is given by
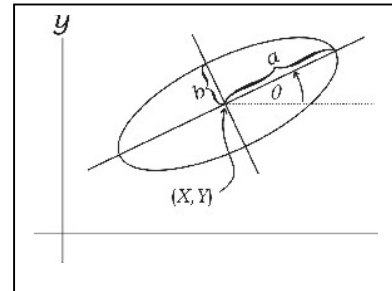

Figure 3. Parameters of the approximation ellipse.

$$A = \frac{\pi}{N^2} \left| \left| \hat{z}_1 \right|^2 - \left| \hat{z}_{-1} \right|^2 \right|. \tag{8}$$

For simple perforations this value of θ is taken as the mean orientation of the shape with respect to the horizontal. For typical holes in plates the area A underestimates the area of the shape by up to 40 %. Instead, the boundary tracing method has been adapted to calculate the total area of the shape in units of pixel-squared with little extra computation time, instead of using A.

Although not relevant to the current application, it is worth mentioning that Fourier shape description can be used particularly well for shape comparison, since it can extract parameters of a closed contour that are invariant under translation, rotation, reflection, starting point of digitization, and order (clockwise or counter clockwise) of digitization. If required, scale invariance may also be enforced by scaling the parameters for example by the square root of the area of the approximation ellipse.

CLASSIFICATION OF IRREGULAR HOLES IN WITNESS PLATES

Irregular holes are those which have large components in the higher frequency modes. Relatively large amplitudes in the second modes already imply significant deviation from an ellipse, therefore the sum of the moduli of higher frequency coefficients for $m = 2,3,...$ ought to be a measure of the level of irregularity. We therefore calculate the following *irregularity quantifier*

$$S = \frac{1}{N} \sum_{m=2}^{N-2} \hat{z}_m \bar{\hat{z}}_m . \tag{9}$$

However, very small irregular holes are not to be handled separately, i.e. they are simply assumed to be simple perforations, and therefore we also scale by the area of the approximation ellipse, i.e.

$$S' = \frac{1}{NA} \sum_{m=2}^{N-2} \hat{z}_m \bar{\hat{z}}_m , \tag{10}$$

where A is given by (8). For S' above a certain threshold h, the shape is considered irregular and is highlighted for hand separation by the user. For typical holes in witness plates photographed at a resolution of between 1.5 and 3 pixel/mm, selecting h to lie between 2 and 4 appears to give good results. The choice of using S' instead of S as irregularity quantifier, causes the algorithm to classify fairly large holes that are only slightly irregular also as irregular, which is also desirable since all fairly large but slightly irregular holes ought to be inspected visually by the operator.
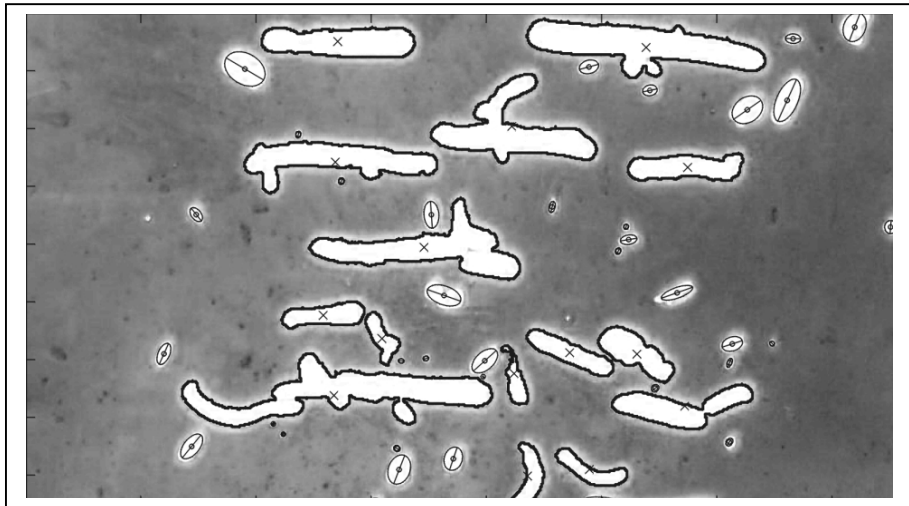
Figure 4.   Results of applying the irregular hole separation. Regular holes are shown with their approximation ellipses. Irregular holes are outlined in black and their edge centroids are denoted by ✕.

Figure 4 shows the results of the method applied to the section of the witness plate in Figure 1 with threshold $h = 4$.

Software was developed that prompts the user to decide on how to handle every irregular hole. The user may opt to simply discard the shape (e.g. for holes on the edge of the plate, or artefacts that were falsely parameterised as holes), or may accept the shape with no alterations (e.g. for fairly large but otherwise regular holes).

Finally the user may decide to cut the shape into overlapping

Figure 5. Results after the user has cut the hole into three supposed single perforations.

patches using a graphical cursor. Figure 5 shows the results after the user has judged the compound perforation to have been caused by three simple perforations, and has cut the relevant shape into three overlapping patches accordingly. Each new single shape is then analysed the normal way.
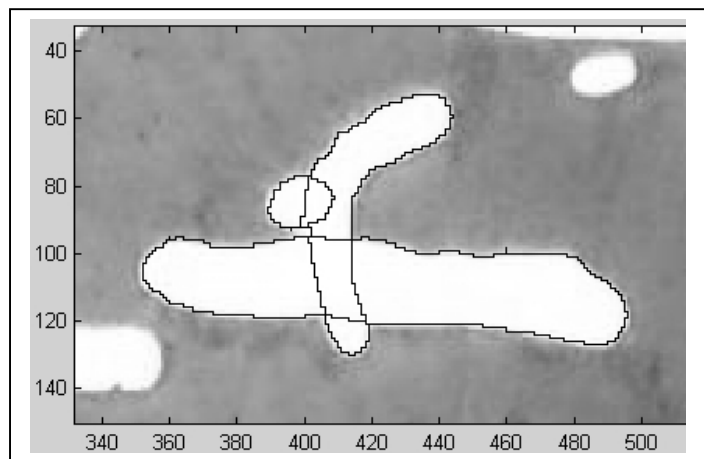
CONCLUSION

In automated data collection from digital images of witness plates, special provision must be made for holes resulting from multiple perforations. The application of Fourier shape analysis presented in this paper is a typical example of how the technique may be used for separating such irregular holes from regular holes. In addition the technique provides an easy means of obtaining the orientation angle for elongated holes.

It is envisaged that in the future analysis of shapes from flash radiographs will also benefit from Fourier shape description techniques. In particular the rotation and translation invariance offered by the Fourier parameters may be useful for classifying shapes into particular classes, for example in radiograph analysis of fragmentation warheads with more that one type of fragment.

REFERENCES

[1] T.E. Carlsson, G. Andersson, A. Helte, B. Janzon, S. Carlsson, J. Lundgren, and H. Örnhed,A new approach for evaluation of flash radiograph images of non-particulated shaped charge jets, *21st International Symposium on Ballistics*, 781-787 (2004)

[2] L.A.Verhagen and J. L. M. J.Th. van Bree, Digital Image Processing Applied to Flash X-Ray Shadowgraphs to Determine Fragment Mass Distribution*, 10th International Symposium on Ballistics* (1987)

[3] C.J.M. van der Wulp, J.H. Meulman, and J.L. Verolme, Digitization of Witness Pack Plates, *19th International Symposium on Ballistics*, 953 – 959 (2001)

[4] R. Schreier, A. Ben-Moshe, M. Markovits, R. Kimmel, M. Moshkovich, and M. Lifshitz, Segmentation of flash radiograph images of ballistic phenomena using the geodesic active contours method, *20th International Symposium on Ballistics*, 933-940 (2002)

[5] http://www.titan-psd.com/html/CommImaging2.htm

[6] R. Gonzales and R. Woods, *Digital Image Processing*, Addison-Wesley Publishing Company (1992)

[7] W.K. Pratt, *Digital Image Processing*, John Wiley & Sons, Inc., New York (1991)

[8] R. Hartley and A. Zisserman, *Multiple View Geometry in Computer Vision*, 2nd ed. ,Cambridge University Press (2003)

[9] F.J.Rohlf and J.W.Archie, A comparison of Fourier methods for the description of wing shape in mosquitoes (Diptera: Culicidae), *Syst. Zool.*, **33**, 302-317 (1984)

[10] A. Blake and M. Isard, *Active Contours*, Springer-Verlag, London (1998)

[11] J. W. Cooley and J.W. Tukey,: An algorithm for the machine calculation of complex Fourier series, *Math. Comput.* **19**, 297–301 (1965)